FIRST DEMONSTRATION OF MeV ELECTRON DIFFRACTION USING THE SUPERCONDUCTING RF PHOTOINJECTOR AT THE HELMHOLTZ-ZENTRUM DRESDEN-ROSSENDORF

R. Niemczyk*[1], L. Stein[1,2], A. Arnold[1], J. M. Klopf[1], U. Lehnert[1], S. F. Maehrlein[1,2], A. Ryzhov[1], J. Teichert[1], E. Uykur[1], A. Wagner[1], S. Winnerl[1], R. Xiang[1]
[1]Helmholtz-Zentrum Dresden-Rossendorf, Dresden, Germany
[2]Technische Universität Dresden, Dresden, Germany

Abstract

Ultrafast electron diffraction (UED) allows for the characterization of structural and electronic dynamics in samples with sub-picosecond resolution. Utilizing a continuous wave photoinjector gives rise to MeV UED at MHz repetition rates, which has the benefits of better temporal resolution, higher beam coherence, higher resolution, and high repetition rates than conventional keV sources. A superconducting radiofrequency (SRF) photoinjector is part of the existing ELBE user facility at the Helmholtz-Zentrum Dresden-Rossendorf (HZDR), delivering electron beams in user operation since 2010. The HZDR is currently planning the Dresden Advanced Light Infrastructure (DALI), a source of THz and IR radiation and positrons. One of DALI's end stations will consist of an MeV UED facility, allowing for pump with IR and THz excitation, and probing with an electron beam, generated by an HZDR-type SRF photoinjector. In this proceeding, we present the first MeV electron diffraction results using the HZDR-type SRF photoinjector at ELBE.

INTRODUCTION

Knowledge of structural and reaction dynamics of matter are key in the fields of biology, chemistry, physics, and material science [1, 2]. Ultrafast electron diffraction (UED) allows to obtain both the structural and electronic dynamics in thin samples with time resolution of a few tens of femtoseconds [3]. When employing a photoinjector as an electron source, UED can be carried out at MeV energies – which comes with the benefits of better time and atomic resolution, and higher coherence. Moreover, if a continuous wave injector is used, a higher bunch repetition rate can be reached.

Helmholtz-Zentrum Dresden-Rossendorf (HZDR) operates the Center for High-Power Radiation Sources ELBE [4]. Here, a superconducting radio-frequency (SRF) linear accelerator accelerates electrons to energies of up to almost 40 MeV. The electron beam drives one of several secondary radiation sources in user operation, among them the infrared free-electron laser (FEL) oscillator FELBE, the superradiant THz source TELBE, or the positron source PELBE. ELBE accommodates a thermionic injector, as well as an SRF photoinjector. Depending on the beam requirements of the secondary radiation source, either the thermionic or the SRF injector is used as the electron source. Here, the thermionic injector is installed in line with the linear accelerator, while the SRF gun is next to it, and connected to the linear accelerator via a transfer dogleg.

As ELBE is in operation for now more than 25 years, HZDR is planning its successor facility: the Dresden Advanced Light Infrastructure DALI [5]. DALI will consist of an SRF linear accelerator driving an IR FEL oscillator, while a second SRF linear accelerator will drive a positron source, a superradiant THz source, and another THz source in an optical klystron scheme, all three in parallel [5]. The IR beam from the FEL oscillator will serve as a seed signal for the optical klystron. DALI will also host an MeV UED facility, with an HZDR-type SRF gun serving as the electron source for the UED instrument. Use of an SRF gun for MeV electron diffraction was first reported in Ref. [6].

This contribution reports the first demonstration of MeV electron diffraction using the SRF gun installed at ELBE. This static experiment allows for gaining hands-on experience with this technique, testing instrumentation and diagnostics, and later benchmark experimental results with simulations [7].

SRF PHOTOINJECTOR

A schematic of the SRF gun-II, which is currently installed at ELBE, is depicted in Fig. 1. The SRF gun consists of a 3.5-cell niobium cavity, which is operating at an RF resonance frequency of 1.3 GHz [8]. The cavity is located in a liquid helium bath to establish superconduction for its op-

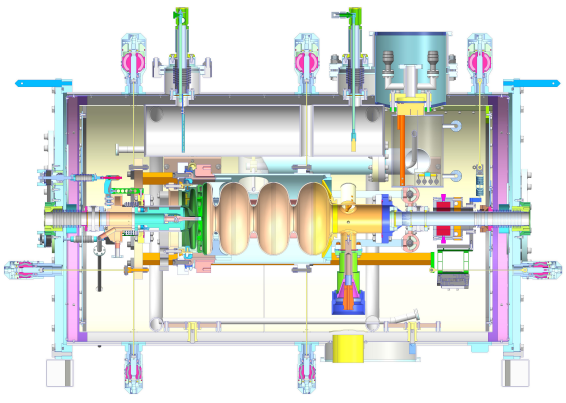

Figure 1: Cross-sectional schematic of the SRF gun-II. The cathode is inserted from the left, where electrons are accelerated within the 3.5-cell cavity and subsequently exit the gun on the right.

* r.niemczyk@hzdr.de

eration. The helium vessel is surrounded by magnetic field shields, isolation vacuum, and also a liquid nitrogen bath to reduce the heat dissipation from the room temperature to the cavity.
The photocathode can be exchanged and is located inside the half-cell. It is electrically isolated and cooled to liquid nitrogen temperature. To suppress multipacting, a DC bias voltage of −5 kV is applied, which corresponds to an accelerating field of 1 MV/m. Copper and magnesium have been used as active cathode materials in the past, while caesium telluride (Cs_2Te) was used most recently [9, 10]. These cathodes have quantum efficiencies as high as 5 % and did not degrade during operation.
The electrons are emitted from the cathode after illumination with a ps-long uv laser pulse, typically with a lateral width of 3.5 mm on the cathode. The accelerating RF field has a peak field strength of 17.9 MV/m, which corresponds to a maximum cathode field of 11.3 MV/m. This allows acceleration up to a kinetic energy of 3.5 MeV. With the SRF gun, either a maximum average current of 1 mA, or a maximum bunch charge of 300 pC can be emitted.

BEAMLINE UPGRADES

The SRF gun ELBE is tightly integrated into its user operation, which usually requires bunch charges of tens to hundreds of pC per electron bunch. For electron diffraction, a beam with a much lower transverse emittance is needed. For this, both the bunch charge and the transverse laser spot size on the cathode were decreased.
The laser spot was reduced by introducing a small pinhole into the path of the photocathode laser, which was imaged onto the cathode using additional imaging lenses. The transmission of light through the small pinhole was also optimized with an additional lens in front of the pinhole. Figure 2 depicts the achieved transverse laser distribution on a camera, which is located at the virtual camera position. Values below

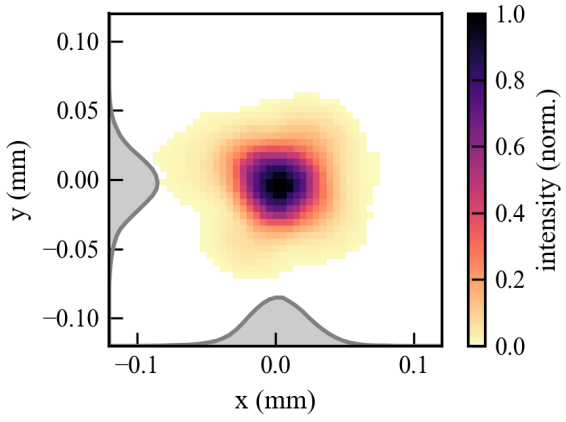

Figure 2: Transverse distribution of the laser spot on the virtual cathode position. A small iris in the laser path, which was imaged onto the cathode, allows to achieve this small spot size. Additionally, the optics was changed to increase the transmission of laser power.

50 µm (FWHM) were achieved in both planes.
While Cs_2Te is well-suited for high-charge operation, metal cathodes are preferable for electron diffraction due to their lower thermal emittance and shorter response time. Although cathode exchange is possible in the SRF gun, it requires warming up the gun cavity — a process too time-consuming to perform during user operation.
As first test samples, single-crystal molybdenum trioxide (MoO_3) and polycrystalline aluminium (Al) was installed on an actuator 2.76 m after the cathode. The aluminium film has a thickness of 31 nm. The samples could be inserted into the beam pipe and rotated in place.
For the detection of the diffraction images scintillating YAG screens, one with a 1.5 mm large hole, were installed 1.9 m downstream the samples. The scintillating light was guided using an in-vacuum mirror and an in-air mirror. A lens imaged the screen position onto an Andor iXon 888 Ultra camera. Dosimeters were used to measure the radiation exposure to the camera, which was only installed for electron diffraction experiments, and removed from the cave afterward. A photograph of the setup is shown in Fig. 3.

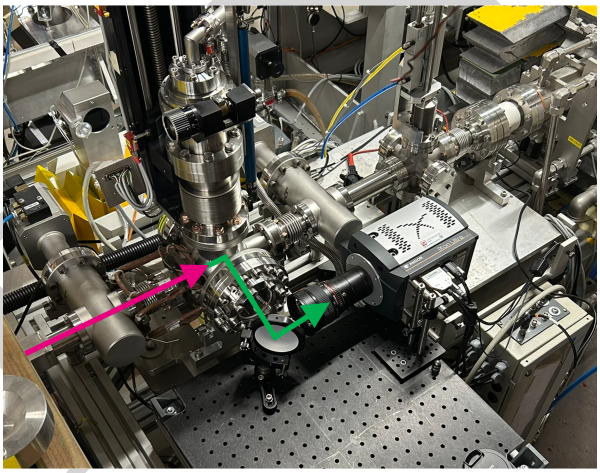

Figure 3: Detection setup for electron diffraction images at ELBE. The diffracted electrons (purple arrow) generate a diffraction pattern on a scintillating YAG screen. The scintillation light (green arrow) is imaged onto an EMCCD camera, mounted on a breadboard.

MHz MeV ELECTRON DIFFRACTION

For the electron diffraction experiments, the gun gradient was slightly reduced, which led to a significant reduction of dark current. With on-crest acceleration the electron beam has a kinetic energy of 3 MeV, which corresponds to an electron wavelength of $\lambda = 0.4$ pm. The laser power was set to emit a charge of 0.6 fC per bunch, while the repetition rate was 13 MHz.
A triplet of quadrupole magnets was used to focus the unscattered beam onto the detector station. The small size of the unscattered beam on the detector screen increases the resolution of the diffraction images. The existing magnetic structure limits the capabilities to achieve a smaller beam size on the sample. In future time-resolved measurements, a

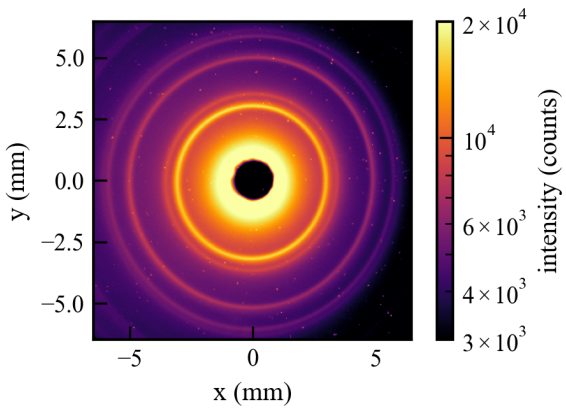

Figure 4: Diffraction image from the aluminium sample. The hole for the main beam is well visible in the center. No noise cut was applied.

pump laser beam will be focused onto the sample to induce a strong excitation in the sample. Then the probe beam has to overlap with the excited part of the sample. In this static demonstration experiment, however, this constrain does not apply yet, making the large electron beam size acceptable. An image of the diffraction signal is depicted in Fig. 4. The image was recorded by integrating the signal for 100 ms. The electron-multiplying capability was not used to obtain this image. When plotting this image, no noise cut or background subtraction was applied; however, the colorscale was limited to a part of the full dynamic range to better resolve the signals. Figure 5 shows the processed diffraction signal strength versus the scattering vector q. The observed diffraction signal matches well with the literature values for aluminium [11].

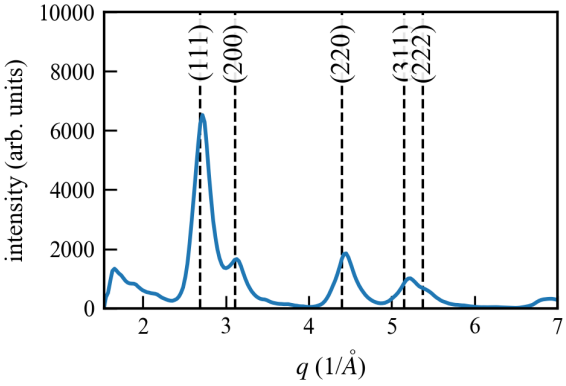

Figure 5: Azimuthally averaged scattering signal versus scattering vector q. The dashed lines show the theoretical expectations for polycrystalline aluminium.

CONCLUSION AND OUTLOOK

An MeV UED facility is foreseen as a powerful user endstation at DALI [5]. To exploit the MHz repetition rates available there, it likewise requires a continuous-wave electron source, such as the HZDR-type SRF gun. We have reported the first demonstration of MHz, MeV-class electron diffraction using this gun — a milestone that provides crucial experience for operating the injector in such applications. As a next step, reducing remnant quadrupole fields in the beamline is foreseen to achieve fully round diffraction rings. Mid-term upgrades could include a collimator, revised electron optics, and a further optimized detection station. Time-resolved measurements will require a dedicated sample chamber, which may be difficult to accommodate given the tight space constraints in the current beamline and the priority of user operation for other ELBE end stations. We will therefore test this in a dedicated UED beamline.

ACKNOWLEDGEMENTS

The authors would like to thank Klaus Floettmann, Alke Meents, Thorsten Kamps, Julian McKenzie, and Xijie Wang for fruitful discussions.

REFERENCES

[1] U. Bergmann *et al.*, "Science and Technology of Future Light Sources: A White Paper", Lawrence Berkeley National Laboratory, Berkeley, California, United States, Dec. 2008.

[2] E. Hall *et al.*, "Future of Electron Scattering and Diffraction", US Department of Energy, Washington, United States, Feb. 2014.

[3] F. Qi *et al.*, "Breaking 50 Femtosecond Resolution Barrier in MeV Ultrafast Electron Diffraction with a Double Bend Achromat Compressor", *Phys. Rev. Lett.*, vol. 124, no. 13, p. 134803, Mar. 2020. doi:10.1103/PhysRevLett.124.134803

[4] M. Helm *et al.*, "The ELBE infrared and THz facility at Helmholtz-Zentrum Dresden-Rossendorf", *Eur. Phys. J. Plus*, vol. 138, no. 158, Feb. 2023. doi:10.1140/epjp/s13360-023-03720-z

[5] "DALI - Dresden Advanced Light Infrastructure, Conceptual Design Report", Helmholtz-Zentrum Dresden-Rossendorf, Dresden, Germany, Sep. 2023.

[6] L. W. Feng *et al.*, "Ultrafast electron diffraction with megahertz MeV electron pulses from a superconducting radio-frequency photoinjector", *Appl. Phys. Lett.*, vol. 107, no. 22, p. 224101, Nov. 2015. doi:10.1063/1.4936192

[7] F. O. Kirchner, S. Lahme, F. Krausz, and P. Baum, "Coherence of femtosecond single electrons exceeds biomolecular dimensions", *New J. Phys.*, vol. 15, no. 6, p. 063021, Jun. 2013. doi:10.1088/1367-2630/15/6/063021

[8] A. Arnold *et al.*, "RF Experience from 6 Years of ELBE SRF-Gun II Operation", in *Proc. SRF'21*, East Lansing, USA, Jun.-Jul. 2021, pp. 477-481. doi:10.18429/JACoW-SRF2021-TUPTEV001

[9] R. Xiang *et al.*, "Cs_2Te normal conducting photocathodes in the superconducting rf gun", *Phys. Rev. ST Accel. Beams*, vol 13, no. 4, p. 043501, Apr. 2010. doi:10.1103/PhysRevSTAB.13.043501

[10] J. Teichert *et al.*, "Successful user operation of a superconducting radio-frequency photo-electron gun with Mg cathodes", *Phys. Rev. Accel. Beams*, vol. 24, no. 3, p. 033401,

Mar. 2021.
doi:10.1103/PhysRevAccelBeams.24.033401

[11] B. J. Siwick *et al.*, "An atomic-level view of melting using femtosecond electron diffraction", *Science*, vol. 302, no. 5649, p. 1382, Nov. 2003.
doi:10.1126/science.1090052